Transport of species in a fibrous media during tissue growth

Samuel LETELLIER
Laboratoire TREFLE site ENSAM, Esplanade des Arts et Métiers, 33405, TALENCE, France
samuel.letellier@bordeaux.ensam.fr

Didier LASSEUX
Laboratoire TREFLE site ENSAM, Esplanade des Arts et Métiers, 33405, TALENCE, France
didier.lasseux@bordeaux.ensam.fr

Azita AHMADI-SENICHAULT
Laboratoire TREFLE site ENSAM, Esplanade des Arts et Métiers, 33405, TALENCE, France
azita.ahmadi-senichault@bordeaux.ensam.fr

Abstract. *Tissue engineering is of major importance in biomedical transplantation techniques. However, some questions subsist as for example the mass transport between each phase (cells, fluid and solid). In a previous paper, a one-equation model was developed in order to model mass transport during in vitro tissue growth using the volume averaging method. Using a dimensionless form of the model and a convenient formulation of the effective dispersion tensor, a numerical resolution of the closure problem is proposed. Some results allowing to validate the numerical tool are presented. This validation is carried out using results available in the literature for 2-D unit cells and under-classes of our model (namely, diffusion, diffusion/reaction and diffusion/advection problems). Finally, we provide some results for the complete model taking into account diffusion, reaction and advection in the three phase system.*

Keywords*. tissue engineering, volume averaging method, diffusion, advection, reaction*

1. Introduction

In this study, we worked in the framework of biotechnologies and more precisely of cartilage tissue engineering. This biomedical technique is relatively recent and has been studied from theoretical (Wood *et al.*, 2001; Wood *et al.*, 2002a; Lasseux *et al.*, 2004), numerical (Ochoa *et al.*, 1986; Galban and Locke, 1999; Wood *et al.*, 2002b) and experimental (Elias *et al.*, 1995; Vunjak-Novakovic *et al.*, 1996; Riesle *et al.*, 1998; Obradovic *et al.*, 1999; Gooch *et al.*, 2001) points of view. Moreover, coupling these different studies, more realistic models describing the complete process of tissue engineering can be derived and allow to predict, for example, the evolution of the cell-mass, or the evolution of the concentration of nutrients (or metabolic products). The aim of the present paper is contribute to this task.

In previous works (Galban and Locke, 1999), the solid phase was neglected or integrated within the cell-phase. However, at least at some stage of the tissue growth, the length-scale of the solid-phase is of the same order of magnitude as the cell colonies. Starting from a microscopic description of the diffusive-advective-reactive problem, Lasseux *et al.* (2004) derived a one-equation model of mass transport of nutrient in a biodegradable porous medium composed of a polymer scaffold. The originality of this study based on up-scaling using a volume averaging procedure is that the model involves diffusion, advection and reaction terms for a three-phase system (Cells (γ-phase), Fluid (β-phase) and Solid (α-phase)). Figure (1) shows the macroscopic region and the averaging volume, V, used for this study, as well as the length-scales of each phase.

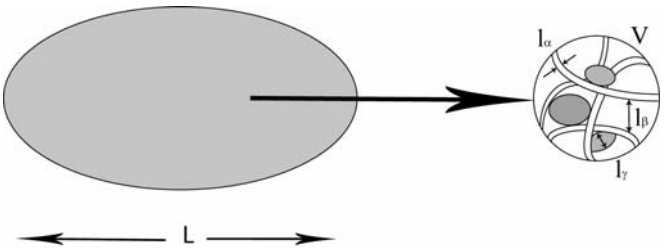

Figure 1. Macroscopic region and averaging volume.

To develop the volume averaged form, the superficial and the intrinsic averages are used (Whitaker, 1999). For a quantity φ_κ associated to the κ-phase, these averages are respectively given by

$$\langle \varphi_\kappa \rangle = \frac{1}{V}\int_{V_\kappa} \varphi_\kappa \, dV \quad , \langle \varphi_\kappa \rangle^\kappa = \frac{1}{V_\kappa}\int_{V_\kappa} \varphi_\kappa \, dV \tag{1}$$

These two quantities are related with the simple relationship

$$\langle \varphi_\kappa \rangle = \varepsilon_\kappa \langle \varphi_\kappa \rangle^\kappa \tag{2}$$

where ε_κ is the volume fraction of the κ-phase

$$\varepsilon_\kappa = \frac{V_\kappa}{V} \tag{3}$$

V_κ being the volume of the κ-phase contained within V. Using L, the length of the unit cell, as the characteristic length, $\|\langle \mathbf{v}_\beta \rangle^\beta\|$ as the reference velocity and $L^2/D_{A\beta}$ as the characteristic time, the dimensionless version of the macroscopic one-equation model takes the form:

$$\left(\varepsilon_\beta + K_{Aeq}\,\varepsilon_\gamma\right)\frac{\partial \{C_A\}}{\partial t} = \mathbf{D}_{\mathbf{Aeff}} : \nabla\nabla \{C_A\} - \varepsilon_\beta Pe \langle \mathbf{v}_\beta \rangle^\beta \cdot \nabla \{C_A\} - k_{Aeff} \{C_A\} \tag{4}$$

where $\{C_A\}$ represents the macroscopic average concentration of nutrients A within the averaging volume, $\langle \mathbf{v}_\beta \rangle^\beta$, is the dimensionless intrinsic average velocity in the β-phase, K_{Aeq} the partition coefficient between the γ-phase and the β-phase at equilibrium for species A, and *Pe* is the cell Peclet number. These last two coefficients are defined below in Eq. (15). The dimensionless effective reaction rate coefficient, k_{Aeff}, and the dimensionless effective dispersion tensor, $\mathbf{D}_{\mathbf{Aeff}}$, are respectively given by:

$$k_{Aeff} = \varepsilon_\gamma K_{Aeq}\, Ki \tag{5}$$

$$\mathbf{D}_{\mathbf{Aeff}} = \left[\begin{array}{c} \varepsilon_\gamma \boldsymbol{\kappa} + \boldsymbol{\kappa} \cdot \left(\frac{1}{V}\int_{A_{\gamma\alpha}} \mathbf{n}_{\gamma\alpha}\mathbf{b}_\gamma \, dA + \frac{1}{V}\int_{A_{\gamma\beta}} \mathbf{n}_{\gamma\beta}\mathbf{b}_\gamma \, dA \right) \\ + \varepsilon_\beta \mathbf{I} + \frac{1}{V}\int_{A_{\beta\alpha}} \mathbf{n}_{\beta\alpha}\mathbf{b}_\beta \, dA + \frac{1}{V}\int_{A_{\beta\gamma}} \mathbf{n}_{\beta\gamma}\mathbf{b}_\beta \, dA \\ - Pe \langle \tilde{\mathbf{v}}_\beta \mathbf{b}_\beta \rangle \end{array}\right] \tag{6}$$

Here, $\mathbf{n}_{\kappa\chi}$ is the unit normal vector directed from the κ-phase toward the χ-phase, $\mathbf{I}$ is the unit tensor, $\tilde{\mathbf{v}}_\beta$ is the dimensionless local spatial deviation of the velocity defined by the classical decomposition $\tilde{\mathbf{v}}_\beta = \mathbf{v}_\beta - \langle \mathbf{v}_\beta \rangle^\beta$ and $\boldsymbol{\kappa}$ is a weighted diffusion coefficient ratio given in Eq. (15).

The effective dispersion tensor involves two closure variables $\mathbf{b}_\gamma$ and $\mathbf{b}_\beta$ that are defined by the following (dimensionless) closure problem:

$$\mathbf{D}_\mathbf{A} : \nabla\nabla \mathbf{b}_\gamma - \varepsilon_\gamma^{-1}\left(\frac{1}{V}\int_{A_{\beta\gamma}} \mathbf{n}_{\gamma\beta} \cdot \mathbf{D}_\mathbf{A} \cdot \left(\nabla \mathbf{b}_\gamma + \mathbf{I}\right) dA \right) - Ki\,\mathbf{b}_\gamma = 0 \quad in\ V_\gamma \tag{7}$$

$$B.C.1: \ \mathbf{n}_{\alpha\gamma} \cdot \mathbf{D}_\mathbf{A} \cdot \nabla \mathbf{b}_\gamma = -\mathbf{n}_{\alpha\gamma} \cdot \mathbf{D}_\mathbf{A} \quad at\ A_{\alpha\gamma} \tag{8}$$

$$\nabla^2 \mathbf{b}_\beta - Pe\,\mathbf{v}_\beta \cdot \nabla \mathbf{b}_\beta - \varepsilon_\beta^{-1}\left(\frac{1}{V}\int_{A_{\beta\gamma}} \mathbf{n}_{\beta\gamma} \cdot \left(\nabla \mathbf{b}_\beta + \mathbf{I}\right) dA \right) = Pe\,\tilde{\mathbf{v}}_\beta \quad in\ V_\beta \tag{9}$$

$$B.C.2: \ \mathbf{n}_{\alpha\beta} \cdot \nabla \mathbf{b}_\beta = -\mathbf{n}_{\alpha\beta} \quad at\ A_{\alpha\beta} \tag{10}$$

$$B.C.3 : \mathbf{n}_{\beta\gamma} \cdot \left(\nabla \mathbf{b}_{\beta} + \mathbf{I}\right) = \mathbf{n}_{\beta\gamma} \cdot \boldsymbol{\kappa} \cdot \left(\nabla \mathbf{b}_{\gamma} + \mathbf{I}\right) \quad at \ A_{\beta\gamma} \tag{11}$$

$$B.C.4 : -\mathbf{n}_{\gamma\beta} \cdot \boldsymbol{\alpha}_{\gamma} \cdot \left(\nabla \mathbf{b}_{\gamma} + \mathbf{I}\right) = \mathbf{b}_{\gamma} - \mathbf{b}_{\beta} \quad at \ A_{\gamma\beta} \tag{12}$$

$$B.C.5 : \mathbf{b}_{\eta}(r + l_i) = \mathbf{b}_{\eta}(r) \quad i = 1,2,3 \ ; \ \eta = \beta, \gamma \tag{13}$$

$$\left\langle \mathbf{b}_{\eta} \right\rangle^{\eta} = 0 \quad \eta = \beta, \gamma \ ; \ \left\langle \mathbf{b}_{\eta} \right\rangle = 0 \quad \eta = \beta, \gamma \tag{14}$$

As in the averaged form of the mass conservation equation, the dimensionless quantities appearing in this closure problem are defined by the following expressions (these definitions are consistent with those used in Ochoa (1988), Quintard and Whitaker (1994) and Neculae *et al.* (2002)):

$$Pe = \frac{\left\| \left\langle \mathbf{v}_{\beta} \right\rangle^{\beta} \right\| L}{D_{A\beta}} \ ; \ Ki = \frac{k_A L^2}{D_{A\beta}} \ ; \ \mathbf{D}_{\mathbf{A}} = \frac{\mathbf{D}_{\mathbf{A}\gamma}}{D_{A\beta}} \ ; \ \boldsymbol{\alpha}_{\gamma} = \frac{\mathbf{D}_{\mathbf{A}\gamma}}{\alpha_A L} \ ; \ \boldsymbol{\kappa} = K_{Aeq} \mathbf{D}_{\mathbf{A}} \tag{15}$$

where $\mathbf{D_{A\gamma}}$ is the diffusion tensor of species A within the γ-phase ($m^2.s^{-1}$) resulting from another up-scaling, $D_{A\beta}$ the diffusion coefficient of species A in the β-phase, α_A the interfacial mass transfer coefficient for species A ($m.s^{-1}$), k_A the reaction rate coefficient of species A (s^{-1}). Note that $\mathbf{D_{A\gamma}}$ (and $\mathbf{D_A}$) are considered as diagonal ones here.

To test this macroscopic model, comparisons with experimental data on the evolution of the macroscopic concentration would be necessary. However, the macroscopic dispersion tensor must be known for a given configuration. The present work provides a solution algorithm of the closure problem in order to compute $\mathbf{D_{Aeff}}$. Section 2 of this paper deals with the reformulation of the closure problem in a more tractable form, providing an alternative convenient expression of the dispersion tensor. The numerical method and algorithm used to solve this problem are also detailed, the validation of which is reported in section 3. To do so, data extracted from the literature are used corresponding to cases that can be considered as under-classes of the present model, namely the pure diffusion problem, the reaction-diffusion problem and the advection-diffusion problem, all being considered in a two-phase (or region) system. Finally, in section 4, results obtained for the full process in a three-phase system are presented.

2. Numerical solution of the closure problem

2.1. Reformulation of the closure problem and the effective dispersion tensor

In order to simplify the expression of the dimensionless dispersion tensor (Eq. (6)), we introduce two variables expressed by

$$\mathbf{u}_{\beta} = \frac{1}{V} \int_{A_{\beta\gamma}} \mathbf{n}_{\beta\gamma} \cdot \left(\nabla \mathbf{b}_{\beta} + \mathbf{I}\right) dA \tag{16}$$

$$\mathbf{u}_{\gamma} = \frac{1}{V} \int_{A_{\beta\gamma}} \mathbf{n}_{\gamma\beta} \cdot \mathbf{D}_{\mathbf{A}} \cdot \left(\nabla \mathbf{b}_{\gamma} + \mathbf{I}\right) dA \tag{17}$$

Moreover, according to the boundary condition (11) and the definition of $\boldsymbol{\kappa}$ (Eq. (15)), $\mathbf{u_\beta}$ and $\mathbf{u_\gamma}$ can be related by the following relationship

$$\mathbf{u}_{\beta} = -K_{Aeq} . \mathbf{u}_{\gamma} \tag{18}$$

Finally, we decompose the closure variables according to

$$\mathbf{b}_{\eta} = \mathbf{d}_{\eta} + B_{\eta} \mathbf{u}_{\beta} \quad \eta = \beta, \gamma \tag{19}$$

Using such a decomposition, two problems independent of $\mathbf{u_\beta}$ and $\mathbf{u_\gamma}$ are obtained. These problems must be solved on a unit cell representative of a periodic porous medium. The issue concerning periodic boundary conditions has been thoroughly discussed elsewhere (Whitaker, 1999).

Problem 1:

$$\mathbf{D_A}:\nabla\nabla\,\mathbf{d}_\gamma - Ki\,\mathbf{d}_\gamma = 0 \;\; in\; V_\gamma \tag{20}$$

$$B.C.1:\ \mathbf{n}_{\alpha\gamma}\cdot\mathbf{D_A}\cdot\nabla\mathbf{d}_\gamma = -\mathbf{n}_{\alpha\gamma}\cdot\mathbf{D_A} \quad at\ A_{\alpha\gamma} \tag{21}$$

$$\nabla^2\mathbf{d}_\beta - Pe\,\mathbf{v}_\beta\cdot\nabla\mathbf{d}_\beta = Pe\,\widetilde{\mathbf{v}}_\beta \quad in\ V_\beta \tag{22}$$

$$B.C.2:\ \mathbf{n}_{\alpha\beta}\cdot\nabla\mathbf{d}_\beta = -\mathbf{n}_{\alpha\beta} \quad at\ A_{\alpha\beta} \tag{23}$$

$$B.C.3:\ \mathbf{n}_{\beta\gamma}\cdot\left(\nabla\mathbf{d}_\beta + \mathbf{I}\right) = \mathbf{n}_{\beta\gamma}\cdot\boldsymbol{\kappa}\cdot\left(\nabla\mathbf{d}_\gamma + \mathbf{I}\right) \quad at\ A_{\beta\gamma} \tag{24}$$

$$B.C.4:\ -\mathbf{n}_{\gamma\beta}\cdot\boldsymbol{\alpha}_\gamma\cdot\left(\nabla\mathbf{d}_\gamma + \mathbf{I}\right) = \mathbf{d}_\gamma - \mathbf{d}_\beta \quad at\ A_{\gamma\beta} \tag{25}$$

$$B.C.5:\ \mathbf{d}_\eta(r + l_i) = \mathbf{d}_\eta(r) \quad i = 1,2,3\ ;\ \eta = \beta,\gamma \tag{26}$$

$$\left\langle\mathbf{d}_\eta\right\rangle^\eta = 0 \quad \eta = \beta,\gamma\ ;\ \left\langle\mathbf{d}_\eta\right\rangle = 0 \quad \eta = \beta,\gamma \tag{27}$$

Problem 2:

$$\mathbf{D_A}:\nabla\nabla B_\gamma - KiB_\gamma = -\varepsilon_\gamma^{-1}K_{Aeq}^{-1} \quad in\ V_\gamma \tag{28}$$

$$B.C.1:\ \mathbf{n}_{\alpha\gamma}\cdot\mathbf{D_A}\cdot\nabla B_\gamma = 0 \quad at\ A_{\alpha\gamma} \tag{29}$$

$$\nabla^2 B_\beta - Pe\,\mathbf{v}_\beta\cdot\nabla B_\beta = \varepsilon_\beta^{-1} \quad in\ V_\beta \tag{30}$$

$$B.C.2:\ \mathbf{n}_{\alpha\beta}\cdot\nabla B_\beta = 0 \quad at\ A_{\alpha\beta} \tag{31}$$

$$B.C.3:\ \mathbf{n}_{\beta\gamma}\cdot\nabla B_\beta = \mathbf{n}_{\beta\gamma}\cdot\boldsymbol{\kappa}\cdot\nabla B_\gamma \quad at\ A_{\beta\gamma} \tag{32}$$

$$B.C.4:\ -\mathbf{n}_{\gamma\beta}\cdot\boldsymbol{\alpha}_\gamma\cdot\nabla B_\gamma = B_\gamma - B_\beta \quad at\ A_{\gamma\beta} \tag{33}$$

$$B.C.5:\ B_\eta(r + l_i) = B_\eta(r) \quad i = 1,2,3\ ;\ \eta = \beta,\gamma \tag{34}$$

$$\left\langle B_\eta\right\rangle^\eta = 0 \quad \eta = \beta,\gamma\ ;\ \left\langle B_\eta\right\rangle = 0 \quad \eta = \beta,\gamma \tag{35}$$

Once the two above problems are solved, one can compute $\mathbf{b}_\eta$ according to

$$\mathbf{b}_\eta = \mathbf{d}_\eta - B_\eta\frac{\left\langle\mathbf{d}_\beta\right\rangle^\beta}{\left\langle B_\beta\right\rangle^\beta} \quad \eta = \beta,\gamma \tag{36}$$

To obtain this last relationship, we have made use of the first of Eq. (14). Moreover, to simplify the computation of the dispersion tensor, another form of Eq. (6) is derived. To do so, the averaging theorem, relating the average of a gradient to the gradient of the average (Howes and Whitaker, 1985), is used.

$$\left\langle\nabla\mathbf{b}_\eta\right\rangle = \nabla\left\langle\mathbf{b}_\eta\right\rangle + \frac{1}{V}\int_{A_{\alpha\eta}}\mathbf{n}_{\eta\alpha}\cdot\mathbf{b}_\eta dA + \frac{1}{V}\int_{A_{\mu\eta}}\mathbf{n}_{\eta\mu}\cdot\mathbf{b}_\eta dA \quad \eta = \beta,\gamma \quad \mu = \gamma,\beta \quad \mu \neq \eta \tag{37}$$

In addition, according to Eq. (14), $\langle\mathbf{b}_\eta\rangle=0$ eliminating its gradient in Eq. (37). The effective dispersion tensor can therefore be rewritten as:

$$\mathbf{D}_{\mathbf{Aeff}} = \varepsilon_\gamma \boldsymbol{\kappa} + \varepsilon_\beta \mathbf{I} + \boldsymbol{\kappa} \cdot \left\langle \nabla \mathbf{b}_\gamma \right\rangle + \left\langle \nabla \mathbf{b}_\beta \right\rangle + Pe \left\langle \tilde{\mathbf{v}}_\beta \mathbf{b}_\beta \right\rangle \tag{38}$$

2.2. Algorithm

Our numerical approach developed in this work makes use of the finite volume discretisation method over a Cartesian structured grid. In order to solve closure problems (Eqs. (20) to (35)), the local (or microscopic) velocity field must be known. The computation of the velocity can be considered independently and can be performed on the basis of the Stokes or Navier-Stokes model. In this work, the Navier-Stokes problem is solved using an artificial compressibility algorithm and a modified QUICK scheme to treat the non-linear term. The closure problems to be solved have essentially a diffusion/convection/reaction structure. A staggered grid is employed (B_η and $\mathbf{d}_\eta$ are located at cell centres while velocities are given on cell faces) and convective terms are treated with a first order upstream scheme while the diffusive ones are discretized using a standard second order centred scheme. Appropriate discretization of the boundary conditions is used to ensure a second order approximation at the $A_{\beta\gamma}$, $A_{\alpha\gamma}$ $A_{\alpha\beta}$ interfaces. Because of the structure of the problem, the linear system obtained is not necessarily symmetric and is solved by a Stabilized Bi-Conjugate Gradient (Bi-CGSTAB) method.

3. Validation

Before using the program in its complete configuration (namely, three phases implying diffusion, reaction and advection), we compared results for simpler cases available in the literature. These configurations can all be considered as particular cases of our general formulation.

3.1. Diffusion problem

First, the pure diffusion problem was studied in order to validate the code. To do so, we used results given by Quintard and Whitaker (1987). In their work, a model for the determination of the macroscopic permeability tensor for a single phase flow in a heterogeneous medium composed of two regions was developed. This problem is equivalent to ours while setting Ki=0, $\boldsymbol{\alpha}_\gamma$=**0**, and Pe=0 in the initial problem given by Eqs. (7) to (14) where integral terms can be easily discarded and in which circumstances $\mathbf{b}_\eta$=$\mathbf{d}_\eta$. The expression of our dimensionless effective dispersion tensor (introducing the parameters above and considering a fluid-phase and a "cell"-phase) is also equivalent to the one of the permeability tensor derived by Quintard and Whitaker. Figure (2) shows the configuration of the unit cell used for comparison as well as the results plotted for different values of ε_β.

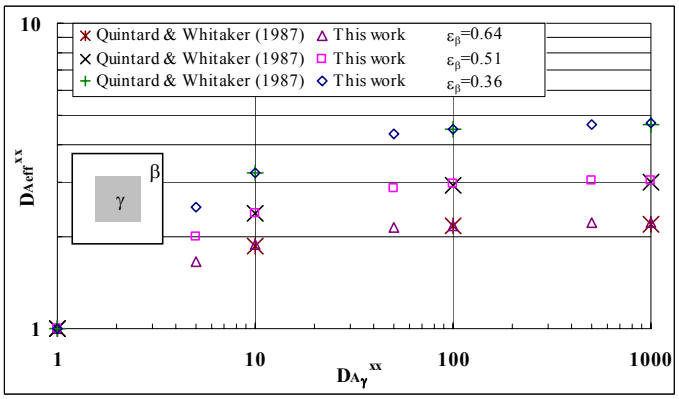

Figure 2. Configuration of the unit cell used for the pure diffusion problem and comparison between results given by Quintard and Whitaker (1987) and ours. The grid was of 40×40.

According to Figure (2), we can notice that our results are in excellent agreement with those in the cited reference. Moreover, as indicated by Quintard and Whitaker, the longitudinal component of $\mathbf{D}_{\mathbf{Aeff}}$ tends to a limit value for a given volume fraction for large values of $\mathbf{D}_{\mathbf{A}}{}^{\mathbf{xx}}$.

3.2. Diffusion-reaction problem

A problem identical to the one considered in this work without convection and with no solid phase was treated by Ochoa (1988). The closure problem obtained by this author was solved in this reference on the unit cell of Fig. (3) for ε_β=0.64; 0.51; 0.36 using a Finite Difference Method (FDM) and a Boundary Element Method (BEM) for ε_β=0.64; 0.36.

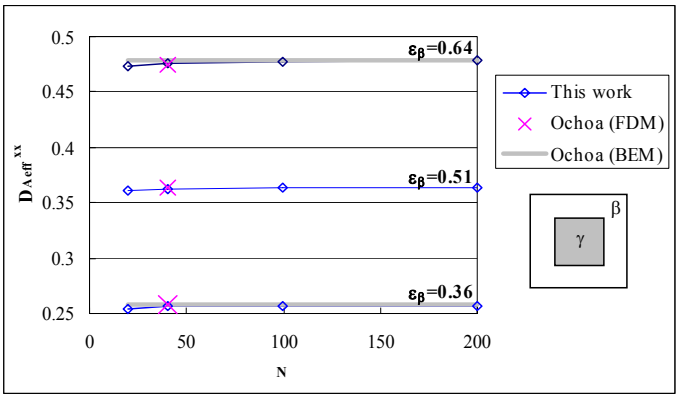

Figure 3. Comparison of results given by Ochoa and ours. Ki=2.78 10^{-3}, $\mathbf{D_A}$=2**I**, α_γ=10**I**, $\boldsymbol{\kappa}$=**I**, K_{Aeq}=0.5.

In Figure (3), we have reported the x component of $\mathbf{D_{Aeff}}$ as a function of the number of grid blocks in each direction. We have also represented by a line Ochoa's results obtained with the BEM and 200 elements. Again, agreement between our results and data available in the above mentioned reference is very satisfactory. For instance, there is less than 1% error between our results for a grid of 200×200 and Ochoa's ones obtained with the BEM.

3.3. Diffusion-advection problem

Here, we treat the classical problem of dispersion of a tracer within a fluid saturating a homogeneous porous medium. Results to this problem were provided by Quintard and Whitaker (1994) on a model system for which the unit cell is represented in the inset of Fig. (4). In such a case, it is sufficient to set ε_γ=0. As shown in Fig. (4), the xx component of the dimensionless effective dispersion tensor follows a classical trend as a function of the cell Peclet number. Moreover, one can note that our results are in perfect agreement with those of this reference.

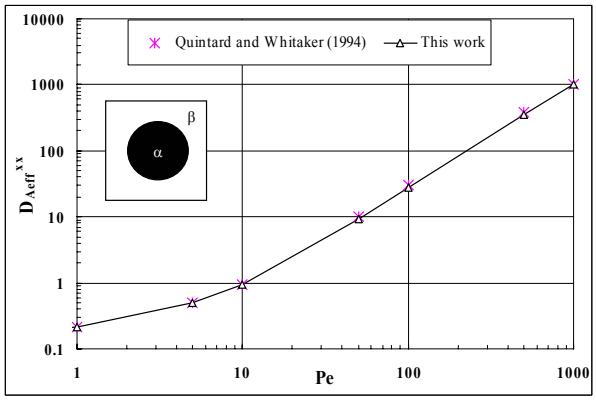

Figure 4. Longitudinal component of $\mathbf{D_{Aeff}}$ as a function of the cell Peclet number, Pe. 100x100 grid blocks

4. Results

In this section, we present numerical results obtained from the solution of closure problems given by Eqs. (20) to (35) computed on a two-dimensional periodic unit-cell shown in the inset of Fig. (6a). In each case, the solid (α)-phase is surrounded by the cell (γ)-phase, and limit cases correspond to the presence of either the solid- or the cell-phase only.

4.1. Influence of the cell Peclet number and of the reaction term

The influence of both Pe and Ki is investigated keeping $\varepsilon_\alpha+\varepsilon_\gamma$ constant and equal to 0.64. First, as shown in Fig. (6), one can see that the longitudinal component of the effective dispersion tensor follows a classical trend as a function of the cell Peclet number. Moreover, the three sets of simulations performed with ε_α=0, ε_α =0.64 and ε_α=0.16, indicate that, for the values of the parameters used here and a given Peclet number, the macro-scale dispersion weakly depends on the respective values of ε_α and ε_γ when the fluid volume fraction remains constant. The slight increase of D_{Aeff}^{xx} with ε_γ at low Peclet numbers can be attributed to diffusion occurring in this phase.

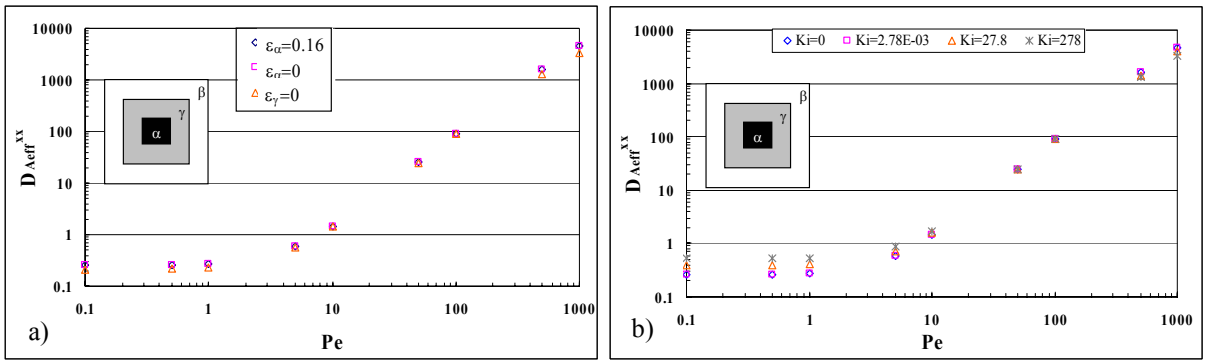

Figure 6. Macroscopic longitudinal dispersion coefficient as a function of *Pe* a) for three different values of ε_α (0, 0.64 and 0.16) *Ki*=2.78 10^{-3}, $\mathbf{D_A}$=2**I**, $\boldsymbol{\alpha_\gamma}$=10**I**, **κ**=**I**, K_{Aeq}=0.5 b) for four values of *Ki* (0, 2.78 10^{-3}, 27.8 and 278) and ε_α=0.16. 40×40 grid blocks.

The dependency of D_{Aeff}^{xx} upon the kinetic number while varying *Pe* is more complex as indicated in Fig. (6b). For *Pe* smaller than 10, D_{Aeff}^{xx} increases when *Ki* increases whereas for *Pe* larger than about 100, on can observe that this effective dispersion coefficient decreases, although less significantly, when *Ki* increases.

4.2. Influence of volume fractions on the dispersion tensor

In this part of the work, the influence of the volume fraction of each phase on the macroscopic longitudinal dispersion is studied. This is performed for three different Peclet numbers (10^{-2}, 1 and 10^2) and results of D_{Aeff}^{xx} are represented versus cell and solid volume fractions in Fig. (7).

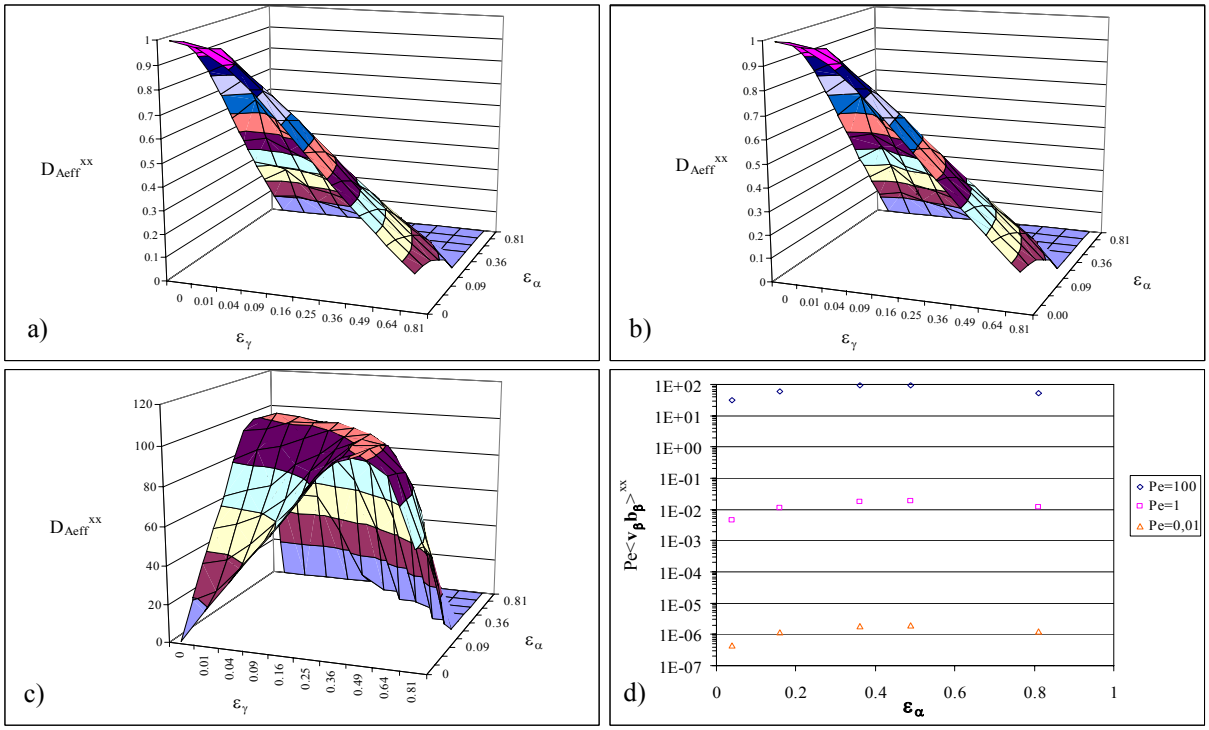

Figure 7. D_{Aeff}^{xx} represented as a function of the solid (ε_α) and cell (ε_γ) phase volume fractions. (a) *Pe*=0.01, (b) *Pe*=1 and (c) *Pe*=100. (d) Values of the longitudinal hydrodynamic dispersion term as a function of ε_γ and *Pe*. *Ki*=2.78 10^{-3}, $\mathbf{D_{A\gamma}}$=2**I**, $\boldsymbol{\alpha_\gamma}$=10**I**, **κ**=**I**, K_{Aeq}=0.5. 200x200 grid blocks

For *Pe*=0.01 and 1 (Figs. (7a) and (7b)), the longitudinal dispersion coefficient decreases, as expected, when the fluid volume fraction decreases. However, for *Pe*=100 (Fig. (7c)), one can clearly observe that D_{Aeff}^{xx} exhibits an

extremum which occurs for ε_β close to 0.5. This trend is due to the contribution of the hydrodynamic dispersion represented by the term $Pe\langle \mathbf{v}_\beta \mathbf{b}_\beta \rangle$ in the macroscopic dispersion tensor. In (Fig (7d)), we have represented the longitudinal part of the hydrodynamic dispersion as a function of ε_α (ε_γ was kept equal to 0) for the three values of *Pe* considered here. While this term always exhibits a "bell-shape" dependence upon ε_α with an extremum at $\varepsilon_\beta \approx 0.5$, it remains small compared to the effective diffusion (including molecular diffusion and tortuosity effects) part of the macro-scale dispersion tensor when *Pe* remains smaller than or of the order of unity. However, for larger values of *Pe* (100 for instance), convection is dominant and the hydrodynamic part is the major contribution in the macroscopic dispersion explaining the behaviour reported in Fig. (7c).

5. Conclusion

In this work, we developed a numerical tool to solve the closure problem associated to the macroscopic one-equation model derived earlier (Lasseux *et al.,* 2004) describing an advection/diffusion/reaction problem in homogeneous porous media involving three distinct phases (a solid phase, a fluid phase and a cell-growing phase) as encountered during in vitro tissue growth. After reformulating both the closure problems and the expression of the effective dispersion tensor in more tractable dimensionless forms, the numerical procedure was presented. It was first successfully validated on the basis of three different problems documented in the literature and representing special cases of a more general one envisaged here. In a second step, the numerical procedure was used to compute the effective dispersion tensor for the complete three-phase problem and illustrative results were provided for simple model 2D periodic unit cells. The dependence of the longitudinal effective dispersion tensor upon some of the physical dimensionless parameters like the cell Peclet number, the kinetic number and volume fractions was investigated. Future work will consist in the association of the present effective dispersion coefficient estimation to numerical growth simulations providing a complete set of numerical analysis of the whole process that could be further compared to direct observations of laboratory experiments.

6. References

Elias, C. B., Desai, R. B., Patole, M. S., Joshi, J. B., Mashelkar, R. A., 1995, "Turbulent shear stress – Effect on mammalian cell culture and measurement using laser Doppler anemometer", Chemical Engineering Science, Vol.50, pp. 2431-2440.

Galban, C. J., and Locke, B. R., 1999, "Analysis of cell growth kinetics and substrate diffusion in polymer scaffold", Biotechnology and Bioengineering, Vol.65, No. 2, pp. 121-132.

Gooch, K. J., Kwon, J. H., Blunk, T., Langer, R., Freed, L. E. and Vunjak-Novakovic, G., 2001, "Effects of mixing intensity on tissue-engineered cartilage", Biotechnology and Bioengineering, Vol.72, No. 4, pp.402-407.

Lasseux, D., Ahmadi, A., Cleis, X. and Garnier, J., 2004, "A macroscopic model for species transport during in vitro tissue growth obtained by the volume averaging method", Chemical Engineering Science, Vol.59, pp. 1949-1964.

Neculae, A., Goyeau, B., Quintard, M. and Gobin, D., 2002, "Passive dispersion in dentritic structures", Materials Science and Engineering A, Vol. 323, pp. 367-376.

Obradovic, B., Meldon, J. H., Freed, L. E. and Vunjak-Novakovic, G., 1999, "Glycosaminoglycan deposition in engineered cartilage: experiments and mathematical model", A.I.Ch.E. Journal, Vol.46, No. 9, pp.1860-1871.

Ochoa, J. A., Stroeve P. and Whitaker, S., 1986, "Diffusion and reaction in cellular media", Chemical Engineering Science, Vol.41, No. 12, pp. 2999-3013.

Ochoa, J. A., 1988, "Diffusion and reaction in heterogeneous media", PhD-Thesis, University of California, Davvis.

Quintard, M. and Whitaker, S., 1987, "Single phase flow in porous media: the effect of local heterogeneities", Journal of Theoretical and Applied Mechanics, Vol.6, No. 5, pp. 691-726.

Quintard, M. and Whitaker, S., 1994, "Convection, dispersion and interfacial transport of contaminants: Homogeneous porous media", Advances in Water Ressources, Vol.17, pp. 221-239.

Riesle, J., Hollander, A. P., Langer, R., Freed, L. E. and Vunjak-Novakovic, G., 1998, "Collagen in tissue-engineered cartilage: types, structure and crosslinks", Journal of Cellular Biochemistry, Vol.71, pp. 313-327.

Vunjak-Novakovic, G., Freed, L. E., Biron, R. J. and Langer, R., 1996, "Effects of mixing on the composition and morphology of tissue engineered cartilage", A.I.Ch.E. Journal, pp. 850-860.

Wood, B., Quintard, M. and Whitaker, S., 2001, "Methods for predicting diffusion coefficients in biofilms and cellular systems", Methods in Enzymology, Vol. 337, pp. 319-338.

Wood, B., Quintard, M., Golfier, F. and Whitaker, S., 2002a, "Biofilms in porous media: development of macroscopic transport equations via volume averaging with closure", Computational Methods in Water Ressources, Vol.2, pp. 1195-1202.

Wood, B., Quintard, M. and Whitaker, S., 2002b, "Calculation of effective diffusivities for biofilms and tissues", Biotechnology and Bioengineering, Vol.77, No. 5, pp. 495-516.

Whitaker, S., 1999, "The method of volume Averaging", Theory and Applications of Transport in porous media, Kluwer Academic Publishers, Vol.13.